

# ABSTRACT

Title of dissertation: MEASURING TOPOLOGY OF BECS  
IN A SYNTHETIC DIMENSIONAL LATTICE

Dina Genkina  
Doctor of Philosophy, 2019

Dissertation directed by: Professor Ian Spielman  
Joint Quantum Institute,  
National Institute of Standards and Technology,  
and  
Department of Physics, University of Maryland

We describe several experiments performed on a two species apparatus capable of producing Bose-Einstein condensates (BECs) of  $^{87}\text{Rb}$  and degenerate Fermi gases (DFGs) of  $^{40}\text{K}$ .

We first describe computational results for observed optical depths with absorption imaging, in a regime where imaging times are long enough that recoil-induced detuning introduces significant corrections. We report that the observed optical depth depends negligibly on the cloud shape. We also find that the signal-to-noise(SNR) ratio for low atom numbers can be significantly improved by entering this regime and applying the appropriate corrections. We take advantage of this SNR improvement in our subsequent experiment colliding two clouds of  $^{40}\text{K}$  for different values of background magnetic field in the vicinity of a Feshbach resonance. We directly imaged the fraction of scattered atoms, which was low and difficult to detect. We used this method to measure the resonance location to be  $B_0 = 202.06(15)$

Gauss with width  $\Delta = 10.5$  Gauss, in good agreement with accepted values.

Next, we describe experiments creating an elongated effectively 2D lattice for a BEC of  $^{87}\text{Rb}$  with non-trivial topological structure using the technique of synthetic dimensions. We set up the lattice by applying a 1D optical lattice to the atoms along one direction, and treating the internal spin states of the atoms as lattice sites in the other direction. This synthetic direction is therefore very short, creating a strip geometry. We then induce tunneling along the synthetic direction via Raman coupling, adding a phase term to the tunneling coefficient. This creates an effective magnetic flux through each lattice plaquette, in the Hofstadter regime, where the flux is of order the flux quantum  $h/e$ . We detect the resulting eigenstate structure, and observe chiral currents when atoms are loaded into the central synthetic site. We further launch analogues of edge magnetoplasmons and image the resulting skipping orbits along each edge of the strip.

We then applied a force along the real dimension of the 2D lattice and directly imaged the resulting motion in the transverse, synthetic, direction. We performed these measurements with 3 and 5-site width lattices along the synthetic direction. We used these measurements to identify the value of the Chern number, the topological invariant in 2D, by leveraging the Diophantine equation derived by Thouless, Kohomoto, Nightingale, and den Nijs. We measure Chern numbers with typical uncertainty of 5%, and show that although band topology is only properly defined in infinite systems, its signatures are striking even in extremely narrow systems.

Measuring topology of BECs in a synthetic dimensions lattice

by

Dina Genkina

Dissertation submitted to the Faculty of the Graduate School of the  
University of Maryland, College Park in partial fulfillment  
of the requirements for the degree of  
Doctor of Philosophy  
2019

Advisory Committee:

Professor Ian Spielman, Chair/Advisor

Professor Mohammad Hafezi, Dean's representative

Professor Steven Rolston

Professor Trey Porto

Professor Christopher Lobb

© Copyright by  
Dina Genkina  
2019



## Acknowledgments

This thesis describes work that was carried out by many people, in a way that the multitude of authors on each of the papers only begins to convey. However, as this is the acknowledgement section of *my* thesis, I will endeavor to thank all the people that guided and supported me during my admittedly long tenure as a graduate student.

I would first and foremost like to thank my adviser, Dr. Ian Spielman, for taking a chance on a lab-averse recovering theorist. Ian's mentorship style was always patient and supportive, but without compromising on standards. Ian would never ask 'why isn't this done?', but instead ask 'how are things going this fine morning?' and offer insight and advice regarding whatever I happened to be working on. He was a role model to aspire to, both in his unique combination of intuition and rigor in physics and his unparalleled coffee consumption.

The first 'trial' semester of my lab work was spent in the RbLi lab at UMD. During that time, I am grateful to have learned from Dan Campbell, who voluntarily took on teaching me about the BEC production process one step every day, and Ryan Price, whose magical skills with all equipment and dark humor got me through that time. When I first joined the NIST lab, I had the great fortune of learning from a team of outstanding postdocs—the 'old guard'—consisting of Lindsey LeBlanc, Ross Williams, and Matthew Beeler. I thank them for an excellent introduction to not only laboratory techniques and the physics under study but also the art of working as a team.

An unparalleled debt of gratitude goes to Lauren Aycock, who shared the lab with me from day one and taught me most of what I know being an experimentalist. She endured my clumsiness and obstinance and continued teaching and supporting me throughout my time at NIST. Beyond the lab, she helped teach me how to drive and pushed me to do my first half-marathon. I cannot imagine what my graduate career would have been like without her. I would also like to thank post-docs Ben Stuhl and Hsin-I Lu for the role they played in my physics training. Ben's enthusiasm for electronic design was infectious and it was an honor to learn from him, be it about about feedback loops or version control. Hsin-I's unparalleled productivity in her own work didn't stop her from taking lots of time to help me in mine. Her wisdom for knowing what the root of a problem is and how to prioritize tasks was invaluable, and she remains a role model for me today.

I am happy to have had the opportunity to work with several visiting German students: Marcell Gall, Max Schemmer, and Martin Link. Marcell excelled in balancing hard, productive work in the lab with fun in his free time, and was generally a joy to be around. Max jumped into the research with a running start, and it was exciting to see what he accomplished in a short amount of time. Martin (Marcell III) forced me to give up my belief that all crossfitters are annoying. It was a pleasure to work with him as well as to exercise and hang out with him.

My later years in the lab were spent with post-doc Mingwu Lu and fellow grad student Alina Escalera. Mingwu has taught me so much about physics, electronics, western philosophy and wine. I am grateful for having the opportunity to learn from him and get to know him. It has been a pleasure to watch Alina grow in the lab,

and to have her understanding support during the rougher parts of paper and thesis writing. Her tenacity and drive are to be admired. I have had few opportunities to spend time with new lab recruits, post-doc Amilson Fritsch and graduate student Graham Reid, but even from our limited interactions I am confident the lab will be left in good hands.

During the writing of this thesis, I have had amazing help and support from my roommates, fellow students and friends. I would like to thank Ana Valdes-Curiel, Paco Salces-Carcoba, Chris Billington, Kristen Voigt and Jon Hoffman for bravely reading through entire chapters of my thesis when I couldn't bare to even look at it. I am extremely grateful to have been part of the amazing living community that is the international house of physicists (IHOP)—it has felt more like a large family than a housing arrangement. I would like to thank both the current IHOPers, Ana, Paco, Chris and Daniel, and notable past IHOPers, Dimitry Trypogeorgos and Rory Speirs. A special thank you to Ana and Paco for unpromptedly feeding me during the final thesis writing days and to them and Chris for continued moral support. Extra special thank you to Kristen, my oldest graduate school friend, for teaching me how to drive, housing me in my times of need, providing me with thesis writing space and support, feeding me uncountable times, and telling me its okay to take a nap.

I would also like to thank Jenna Beckwith for her help at the beginning of my graduate journey, Taylor Cole for her insightful support in the last year that has allowed me to work on my thesis almost without panic, and Dr. Diane Stabler for her constant presence and support throughout my time here and for offering



deceptively simple advice. I would also like to thank the good people at Eli Lilly and Company without whose pioneering research my work would not have been possible.

Above all I would like to thank my family. If it wasn't for my parents' upbringing, graduate school would never have been a possibility for me. I am grateful to them for teaching me all that they have, supporting me throughout my time as a graduate student, but prioritizing my happiness above graduate success. I would like to thank them, my sister Alya, and my brother Pten, for everything.

## Table of Contents

Acknowledgements	ii
List of Tables	vii
List of Figures	viii
4 Absorption Imaging with Recoil Induced Detuning	1
4.1 Recoil-induced detuning . . . . .	1
4.2 Perturbative treatment . . . . .	2
4.3 Stationary atom model . . . . .	3
4.4 Traveling atom model . . . . .	8
4.5 Calibration of saturation intensity . . . . .	9
4.6 SNR optimization . . . . .	12
Bibliography	15

## List of Tables

## List of Figures

1	Recoil induced detuning . . . . .	4
2	Optical depth as a function of probe intensity . . . . .	6
3	Checking stationary atom assumption . . . . .	7
4	Phase space evolution of the atomic cloud . . . . .	10
5	Comparison of stationary and moving atom simulations . . . . .	11
6	Signal-to-noise optimization . . . . .	14

## Chapter 5: Imaging of Scattering Near a Feshbach Resonance

In this chapter, we describe our experiment directly imaging  $s$ -wave scattering halos of  $^{40}\text{K}$  atoms in the vicinity of a Feshbach resonance between the  $|F = 9/2, m_F = -9/2\rangle$  and  $|F = 9/2, m_F = -7/2\rangle$  internal states. We used this data to extract the location of the magnetic fields resonance of 20.206(15) mT and a width of 1.0(5) mT, similar to the accepted values of 20.210(7) mT and 0.78(6) mT [17]. The data presented in this chapter was previously reported in [?].

We first introduced Feshbach resonances in section ???. Although Feshbach resonances are extremely useful for studying and manipulating Fermi gases, their resonant magnetic field values are difficult to predict analytically and are commonly computed via numerical models based on experimental input parameters [?, ?, ?] or determined experimentally [?, ?]. There have been a variety of experimental techniques used to characterize Feshbach resonances, including measuring atom loss due to three-body inelastic scattering, measurement of re-thermalization timescales, and anisotropic expansion of the cloud upon release from a confining potential, all of which infer the elastic scattering cross section from collective behavior of the cloud [?, ?, 5].

Here, we present an alternative technique, where we directly image the enhancement in elastic scattering due to the resonance. We collided pairs of ultra-cold Fermi gases and directly imaged the resulting  $s$ -wave scattered atoms as a function of magnetic field strength. This allowed us to observe the enhancement in scattering without relying on proxy effects. We measured the fraction of atoms scattered

during the collision, and from this fraction deduced the resonant magnetic field and the width of the resonance.

In our dilute DFGs, even with the resonant enhancement of the scattering cross section, only a small fraction of the atoms scattered as the clouds passed through each other. This made direct detection of scattered atoms difficult due to detection uncertainty that disproportionately affected regions of low atomic density. To optimize the signal-to-noise ratio (SNR) for low atom numbers, we absorption imaged with fairly long, high-intensity pulses — a non-standard regime, where the atoms acquired a velocity during imaging and the resulting Doppler-shift was non-negligible. Simulation of the absorption imaging process was necessary for an accurate interpretation of these images, as described in Chapter 4. Using the simulation-corrected images, we extracted the fraction of atoms scattered in our collision experiment.

## 5.1 Experimental procedure

We prepared our degenerate  $^{40}\text{K}$  clouds as described in section ???. After this preparation, we used adiabatic rapid passage (ARP) to transfer the degenerate cloud of  $^{40}\text{K}$  atoms in the  $|F = 9/2, m_F = 9/2\rangle$  state into the  $|F = 9/2, m_F = -9/2\rangle$  state by using a 3.3 MHz rf field and sweeping the bias magnetic field from -0.518 mT to -0.601 mT in 150 ms.

Following the state transfer, we had two versions of the protocol – one for approaching the Feshbach resonance from higher fields and one for approaching it from lower fields. For approaching the resonance from lower fields, we proceeded by ramping the bias magnetic field to 19.05 mT, turning on a 42.42 MHz RF field, and then sinusoidally modulating the bias field at 125 Hz for 0.5 s, with a 0.14 mT amplitude, decohering the  $^{40}\text{K}$  state into an equal mixture of  $|F = 9/2, m_F = -9/2\rangle$  and  $|F = 9/2, m_F = -7/2\rangle$ . For approaching the resonance from higher fields, the same was done at a bias field of 21.71 mT and an RF frequency of 112.3 MHz. The

depolarization allowed the  $^{40}\text{K}$  atoms to interact and re-thermalize, allowing us to further evaporate in the dipole trap [?]. Since  $^{87}\text{Rb}$  is heavier than  $^{40}\text{K}$ , we were able to evaporate the  $^{40}\text{K}$  atoms past the point where  $^{87}\text{Rb}$  atoms were no longer suspended against gravity and had been completely removed. These hyperfine states of  $^{40}\text{K}$  were then used to study their Feshbach resonance.

After evaporation, we ramped the bias field in a two-step fashion to the desired value  $B$  near the Feshbach resonance. We approached the field using our quad coils in Helmholtz configuration (0.19 mT/A, see sec. ??) to bring the magnetic field to a setpoint 0.59 mT away from  $B$ ,  $B - 0.59$  mT when approaching from below and  $B + 0.59$  mT from above. We held the atoms at this field for 100 ms to allow the eddy currents induced by the large quad coils to settle, and then flipped the current of our lower inductance biasZ coils from  $-18$  to  $18$  A (0.017 mT/A, see sec. ??) to quickly change the field the remaining 0.59 mT. This allowed us to study the resonance from both sides without the added losses associated with going through the resonance [10].

Once at the intended bias field, we split the cloud into two spatially overlapping components with opposing momenta and observed scattering as they moved through each other and separated. These counter-propagating components were created using an  $8E_L$  deep near resonant ( $\lambda_L=766.704$  nm) 1-d retro-reflected optical lattice (see sec. ??), where  $E_L = \hbar^2 k_L^2 / 2m_K$  is the lattice recoil energy and  $\hbar k_L = 2\pi\hbar/\lambda$  is the recoil momentum. We rapidly pulsed this lattice on and off with a double-pulse protocol [?,?]. The pulse sequence was optimized to transfer most of the atoms into the  $\pm 2\hbar k_L$  momentum states. Since the initial Fermi gas had a wide momentum spread (in contrast to a BEC, which has a very narrow momentum spread), and the lattice pulsing is a momentum dependent process [?], not all the atoms were transferred into the target momentum states. We experimentally optimized our pulse times to minimize the atoms remaining in the zero momentum state. The

optimized pulse times were 23  $\mu\text{s}$  for the first pulse, 13  $\mu\text{s}$  off interval, and 12  $\mu\text{s}$  for the second pulse [?].

We then released the atoms from the trap and allowed 1 ms for the two opposite momentum states within the cloud to pass through each other, scattering on the way. For the data taken coming from below the Feshbach resonance, we then simply ramped down the field and imaged the atoms. For the data taken coming from above the Feshbach resonance, we ramped the field back up, retreating through the resonance if it had been crossed and thereby dissociating any molecules that were created, and then quickly ramped the field back down and imaged the atoms. We used a 40  $\mu\text{s}$  imaging pulse with  $I_0/I_{\text{sat}} \approx 0.6$  at the center of the probe laser. The total time-of-flight was  $t_{\text{TOF}} = 6.8$  ms.

The magnetic fields produced by the combination of our quad and biasZ coils in the regime of interest were independently calibrated by rf-spectroscopy. We prepared  $^{40}\text{K}$  atoms in the  $|F = 9/2, m_F = -9/2\rangle$  state and illuminated them with an rf-field with some frequency  $\nu_{\text{rf}}$ . We then ramped our high-inductance coils to variable set points, followed by an adiabatic 250  $\mu\text{s}$  ramp of 2.84 mT in the lower inductance coils. We then used Stern-Gerlach and observed the fractional population in the  $|F = 9/2, m_F = -9/2\rangle$  and  $|F = 9/2, m_F = -7/2\rangle$  states as a function of the high-inductance coil current. We fit the fractional population curve to a Gaussian, and considered the center of the fit to be on-resonant, with an uncertainty given by the Gaussian width. We used the Breit-Rabi formula (see sec. ??) to determine the resonant field value at  $\nu_{\text{rf}}$ . We did this for 5 different rf frequencies, and acquired a field calibration with an uncertainty of 0.3 mT, which was included in the listed uncertainty on the center field of the Feshbach resonance.



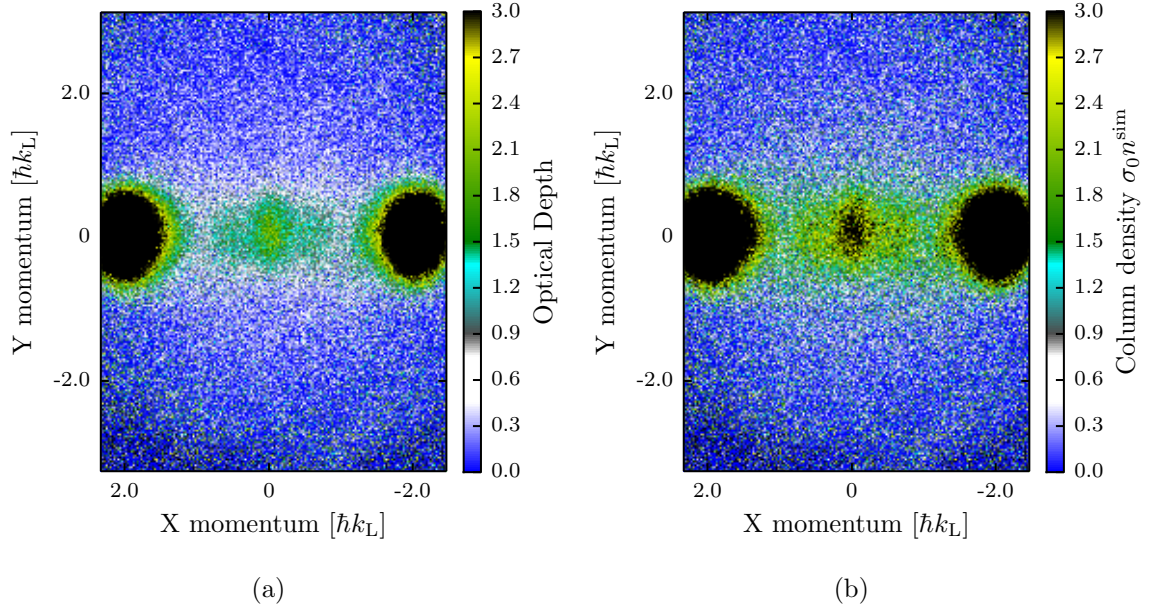


Figure 1: An example of our absorption image after 6.8 ms TOF. The 1-D lattice imparts momentum along  $e_x$ . The two large clouds on the left and right are the atoms in the  $\pm 2k_L$  momentum orders that passed through each other unscattered. The smaller cloud in the center is the atoms that remained in the lowest band of the lattice after pulsing, and thus obtained no momentum. The thin spread of atoms around these clouds is the atoms that underwent scattering. This image was taken coming from below the Feshbach resonance at 20.07 mT. (a) Raw optical depth, (b) atomic column density obtained by comparing to simulated  $ODs$ ,  $\sigma_0 n^{\text{sim}}$

## 5.2 Data analysis

We first processed each image by comparing the observed  $ODs$  to simulations taking into account the recoil induced detuning as described in Chapter 4. An example of images before and after processing are shown in Fig. ???. To improve the signal and mitigate our shot to shot number fluctuations, we took 15 nominally identical images for each data point.

We counted the fraction of atoms that experienced a single scattering event for each of the fifteen images at a given bias magnetic field. Single scattering events are easily identified, as two atoms that scatter elastically keep the same amplitude of momentum, but depart along an arbitrary direction. Therefore, an atom traveling

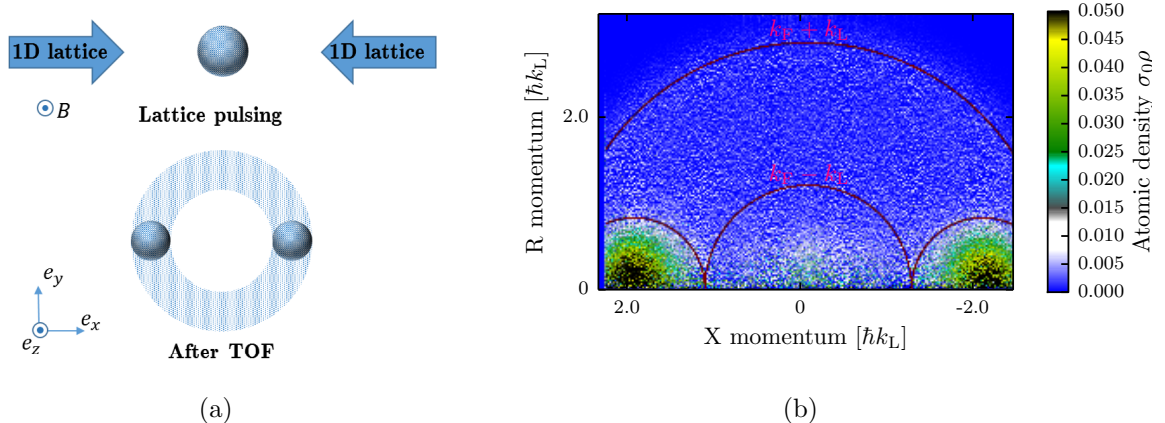


Figure 2: (a) Our experimental setup. After time-of-flight, the two clouds traveling along  $\pm \hat{e}_x$  directions have separated and the atoms that underwent a single scattering event were evenly distributed in a scattering halo around the unscattered clouds. The 1-D lattice defined the axis of cylindrical symmetry. (b) Inverse Abel transformed image. The atoms within the Fermi momentum  $k_F$  of each unscattered cloud center are in the unscattered region and counted towards the total unscattered number. The atoms outside the radius  $k_L - k_F$  but inside  $k_L + k_F$  while also being outside the unscattered region are counted towards the number of single scattered atoms.

at  $2\hbar k_L$  to the right that collides elastically with an atom traveling at  $-2\hbar k_L$  to the left will depart with equal and opposite momenta  $2\hbar k_L$  at an arbitrary angle, and in a time-of-flight image such atoms will lie in a spherical shell, producing the scattering halo pictured in Fig. ??(a).

Absorption images captured the integrated column density along  $e_z$ , a projected 2D atomic distribution. To extract the radial dependence of the 3D distribution from the 2D image, we performed a standard inverse Abel transform. The inverse Abel transform assumes cylindrical symmetry, which was present in our case, with the axis of symmetry along  $e_x$ , defined by the lattice. We neglect the initial asymmetry of the trap, as during time-of-flight the atoms travel far beyond the initial extent of the cloud  $(r_x, r_y, r_z) \approx (45, 48, 15) \mu\text{m}$ , while the cloud width after TOF is  $\approx 82 \mu\text{m}$  in each direction. We thus obtained the atomic distribution  $\rho(r, \theta)$  as a function of  $r$ , the radial distance from the scattering center, and  $\theta$ , the angle

between  $r$  and symmetry axis  $e_x$ , integrated over  $\phi$ , the azimuthal angle around the  $x$  axis.

We then extracted the number of scattered atoms  $N_{\text{scat}}$  as a fraction of the total atom number  $N_{\text{tot}}$  for each image, as shown in Fig. ??(b). The unscattered atom number was the number of atoms in the two unscattered clouds. The number of atoms that underwent a single scattering event was the number of atoms outside the Fermi radius of the unscattered clouds, but inside the arc created by rotating the Fermi momentum  $k_F$  around the original center of the cloud (red arcs in Fig. ??(b)). For both the scattered and unscattered numbers, we accounted for atoms that fell outside the field of view of our camera by multiplying the counted atom number by a factor of the total area as defined by the radii divided by the visible area on the camera. The atoms in the center region were not counted as they were originally in the zero momentum state and could not contribute to the scattering halo under study.

We fit the fraction of scattered atoms versus the total atom number for each of the 15 images taken at the same bias magnetic field to a line constrained to be zero at zero. The slope of this fit was taken to be the value of  $N_{\text{scat}}/N_{\text{tot}}^2$  at that bias magnetic field, and the variance of the fit gave the uncertainty on that data point. This uncertainty reflected our shot to shot number fluctuations, which produced variable atomic densities and thus influence the scattered fraction.

We then deduced the resonant field value  $B_0$  and width of the resonance  $\Delta$ , the parameters in Eq. (??). Since we were in the low energy regime (the atomic momentum was much smaller than the momentum set by the van der Waals length  $k_L + k_F \ll 1/l_{\text{vdW}}$ , and we were well below the p-wave threshold temperature [?]), the scattering cross-section was given by  $\sigma = 4\pi a^2$ .

The scattering cross-section  $\sigma$  gives the probability  $P_{\text{scat}} = \sigma N/A$  that a single particle will scatter when incident on a cloud of atoms with a surface density of

$N/A$ , where  $A$  is the cross-sectional area of the cloud and  $N$  is the number of atoms in the cloud. In our case, each half of the initial cloud, with atoms number  $N_{\text{tot}}/2$ , is incident on the other half. Thus, the number of expected scattering events is  $N_{\text{scat}} = (N_{\text{tot}}/2)\sigma(N_{\text{tot}}/2) = \sigma N_{\text{tot}}^2/4A$ . Assuming  $A$  is constant for all our data, we can define a fit parameter  $b_0 = 4\pi a_{\text{bg}}^2/4A$ , where  $a_{\text{bg}}$  is the background scattering length. We can thus adapt Eq. (??) to obtain the fit function

$$\frac{N_{\text{scat}}}{N_{\text{tot}}^2} = b_0 \left(1 - \frac{\Delta}{B - B_0}\right)^2 + C. \quad (5.1)$$

We found that our imaging noise skewed towards the positive, giving rise to a small background offset. We accounted for this in our fit by including a constant offset parameter  $C$ .

### 5.3 Results

Our final data is presented in Fig. ???. The red curve depicts a best fit of the model given in Eq. (??). The fit parameters we extracted were  $\Delta = 1(5)$  mT,  $B_0 = 20.206(15)$  mT,  $b_0 = 5(3) \times 10^{-3}$  and  $C = 8(1) \times 10^{-4}$ . To obtain the fit, we used data taken by approaching the resonance from above for points above where we expected the resonance to be and data taken approaching the resonance from below for points below. We also excluded from the fit data points very near the resonance, as there the assumption  $\sigma\rho \ll 1$ , where  $\rho$  is the atom number per unit area, is no longer valid and the problem must be treated hydrodynamically.

The accepted values for the  $^{40}\text{K}$  s-wave Feshbach resonance for the  $|9/2, -9/2\rangle$  and  $|9/2, -7/2\rangle$  states are  $B_0 = 20.210(7)$  mT and  $\Delta = 0.78(6)$  mT [17], which is in good agreement with our findings. Some potential sources of systematic uncertainty that we did not account for include scattering with atoms that did not receive a momentum kick from the lattice pulsing or the impact of multiple scattering events.

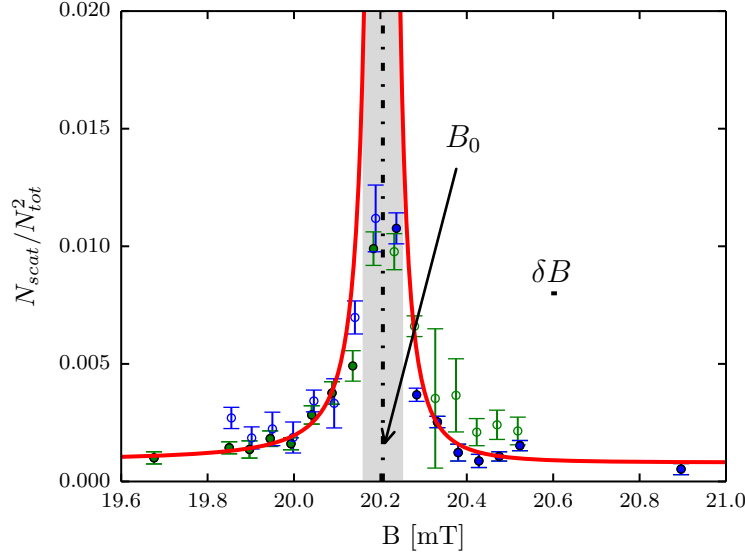


Figure 3: Normalized scattered population plotted versus bias field  $B$ . Green dots represent data taken coming from below the resonance, and blue dots represent the data taken coming from above the resonance. The red curve depicts the best fit, where data coming from above the resonance was used above the resonance and data coming from below the resonance was used below the resonance to create the fit; the unused data points are indicated by hollow dots. The regime where the scattering length is likely large enough for the atoms to behave hydrodynamically is shaded in gray, and data points in that area were also excluded from the fit. Resonant field value  $B_0$  as found in this work and our systematic uncertainty in the bias magnetic field  $\delta B_0$  are indicated.

## Bibliography

- [1] J. R. Ensher, D. S. Jin, M. R. Matthews, C. E. Wieman, and E. A. Cornell. Bose-einstein condensation in a dilute gas: Measurement of energy and ground-state occupation. *Phys. Rev. Lett.*, 77:4984–4987, Dec 1996.
- [2] C.J. Pethick and H. Smith. *Bose-Einstein Condensation of Dilute Gases*. Oxford University Press, Oxford, UK, 2005.
- [3] M. Egorov, B. Opanchuk, P. Drummond, B. V. Hall, P. Hannaford, and A. I. Sidorov. Measurement of  $s$ -wave scattering lengths in a two-component bose-einstein condensate. *Phys. Rev. A*, 87:053614, May 2013.
- [4] W. Ketterle and M. W. Zwierlein. Making, probing and understanding ultracold Fermi gases. In *Ultracold Fermi Gases, Proceedings of the International School of Physics ‘Enrico Fermi’, Course CLXIV*, Varenna, 20-30 June 2006.
- [5] K. M. O’Hara, S. L. Hemmer, M. E. Gehm, S. R. Granade, and J. E. Thomas. Observation of a strongly interacting degenerate Fermi gas of atoms. *Science*, 298(5601):2179–2182, 2002.

- [6] S. Jochim, M. Bartenstein, G. Hendl, J. Hecker Denschlag, R. Grimm, A. Mosk, and M. Weidemüller. Magnetic field control of elastic scattering in a cold gas of fermionic lithium atoms. *Phys. Rev. Lett.*, 89:273202, Dec 2002.
- [7] K. Dieckmann, C. A. Stan, S. Gupta, Z. Hadzibabic, C. H. Schunck, and W. Ketterle. Decay of an ultracold fermionic lithium gas near a feshbach resonance. *Phys. Rev. Lett.*, 89:203201, Oct 2002.
- [8] T. Loftus, C. A. Regal, C. Ticknor, J. L. Bohn, and D. S. Jin. Resonant control of elastic collisions in an optically trapped fermi gas of atoms. *Phys. Rev. Lett.*, 88:173201, Apr 2002.
- [9] C. A. Regal, C. Ticknor, J. L. Bohn, and D. S. Jin. Tuning  $p$ -wave interactions in an ultracold fermi gas of atoms. *Phys. Rev. Lett.*, 90:053201, Feb 2003.
- [10] C. Chin, R. Grimm, P. Julienne, and E. Tiesinga. Feshbach resonances in ultracold gases. *Rev. Mod. Phys.*, 82:1225–1286, 2010.
- [11] M. Greiner, C. A. Regal, and D. S. Jin. Emergence of a molecular Bose-Einstein condensate from a Fermi gas. *Nature*, 426(6966):537–540, 2003.
- [12] M. W. Zwierlein, C. A. Stan, C. H. Schunck, S. M. F. Raupach, S. Gupta, Z. Hadzibabic, and W. Ketterle. Observation of Bose-Einstein condensation of molecules. *Phys. Rev. Lett.*, 91:250401, 2003.
- [13] S. Jochim, M. Bartenstein, A. Altmeyer, G. Hendl, S. Riedl, C. Chin, J. Hecker Denschlag, and R. Grimm. Bose-Einstein condensation of molecules. *Science*, 302(5653):2101–2103, 2003.
- [14] M. Bartenstein, A. Altmeyer, S. Riedl, S. Jochim, C. Chin, J. Hecker Denschlag, and R. Grimm. Collective excitations of a degenerate gas at the bec-bcs crossover. *Phys. Rev. Lett.*, 92:203201, 2004.

- [15] T. Bourdel, L. Khaykovich, J. Cubizolles, J. Zhang, F. Chevy, M. Teichmann, L. Tarruell, S. J. J. M. F. Kokkelmans, and C. Salomon. Experimental Study of the BEC-BCS Crossover Region in Lithium 6. *Phys. Rev. Lett.*, 93:050401, 2004.
- [16] M. W. Zwierlein, C. A. Stan, C. H. Schunck, S. M. F. Raupach, A. J. Kerman, and W. Ketterle. Condensation of pairs of Fermionic atoms near a Feshbach resonance. *Phys. Rev. Lett.*, 92:120403, 2004.
- [17] C. A. Regal, M. Greiner, and D. S. Jin. Observation of resonance condensation of fermionic atom pairs. *Phys. Rev. Lett.*, 92(4), 2004.
- [18] Y.-J. Lin, A. R. Perry, R. L. Compton, I. B. Spielman, and J. V. Porto. Rapid production of  $^{87}\text{Rb}$  bose-einstein condensates in a combined magnetic and optical potential. *Phys. Rev. A*, 79:063631, Jun 2009.
- [19] Karina Jimenez-Garcia. *Artificial Gauge Fields for Ultracold Neutral Atoms*. PhD thesis, Joint Quantum Institute, National Institute of Standards and Technology, and the University of Maryland, 2012.
- [20] Lauren M. Aycock. *Topological excitations in a Bose gas and sexual harassment reported by undergraduate physicists*. PhD thesis, Cornell University, Ithaca, NY, 1 2017.
- [21] Lauren M. Aycock, Hilary M. Hurst, Dmitry K. Efimkin, Dina Genkina, Hsin-I Lu, Victor M. Galitski, and I. B. Spielman. Brownian motion of solitons in a bose-einstein condensate. *Proceedings of the National Academy of Sciences*, 114(10):2503–2508, 2017.
- [22] Christopher J. Foot. *Atomic Physics*. Cambridge University Press, Cambridge, UK, 2002.



- [23] E. A. Donley, T. P. Heavner, F. Levi, M. O. Tataw, and S. R. Jefferts. Double-pass acousto-optic modulator system. *Review of Scientific Instruments*, 76(6):063112, 2005.
- [24] Ryan Price. *Phase transitions in engineered ultracold quantum systems*. PhD thesis, University of Maryland College Park, Digital Repository at the University of Maryland, 6 2016.
- [25] E. Majorana. Atomi orientati in campo magnetico variabile. *Nuovo Cimento*, 9:43–50, Feb 1932.
- [26] C. V. Sukumar and D. M. Brink. Spin-flip transitions in a magnetic trap. *Phys. Rev. A*, 56:2451–2454, Sep 1997.
- [27] D. M. Brink and C. V. Sukumar. Majorana spin-flip transitions in a magnetic trap. *Phys. Rev. A*, 74:035401, Sep 2006.
- [28] J. Catani, P. Maioli, L. De Sarlo, F. Minardi, and M. Inguscio. Intense slow beams of bosonic potassium isotopes. *Phys. Rev. A*, 73:033415, Mar 2006.
- [29] Thomas Uehlinger. A 2-d magneto-optical trap as a high flux source of cold potassium atoms. Master’s thesis, Swiss Federal Institute of Technology Zurich, Zurich, 5 2008.
- [30] E. Pedrozo-Peafiel, F. Vivanco, P. Castilho, R. R. Paiva, K. M. Farias, and V. S. Bagnato. Direct comparison between a two-dimensional magneto-optical trap and a zeeman slower as sources of cold sodium atoms. *Laser Physics Letters*, 13:065501, May 2016.
- [31] K. J. Weatherill, J. D. Pritchard, P. F. Griffin, U. Dammalapati, C. S. Adams, and E. Riis. A versatile and reliably reusable ultrahigh vacuum viewport. *Review of Scientific Instruments*, 80(2):026105, 2009.

- [32] D. Rio Fernandes, F. Sievers, N. Kretzschmar, S. Wu, C Salomon, and F. Chevy.  
Sub-doppler laser cooling of fermionic 40k atoms in three-dimensional gray  
optical molasses. *Europhysics Letters*, 100:63001, Dec 2012.